A screening setup to streamline *in vitro* engineered living material cultures with the host

Krupansh Desai [a,b], Shrikrishnan Sankaran [a], Aránzazu del Campo [a,b], Sara Trujillo [a,c,*]

[a] *INM - Leibniz Institute for New Materials, Campus D2 2, Saarbrücken, 66123, Germany*
[b] *Chemistry Department, Saarland University, Saarbrücken, 66123, Germany*
[c] *Saarland University, Pharma Science Hub (PSH), 66123 Saarbrucken, Germany*

A B S T R A C T

Engineered living materials (ELMs), which usually comprise bacteria, fungi, or animal cells entrapped in polymeric matrices, offer limitless possibilities in fields like drug delivery or biosensing. Determining the conditions that sustain ELM performance while ensuring compatibility with ELM hosts is essential before testing them in vivo. This is critical to reduce animal experimentation and can be achieved through *in vitro* investigations. Currently, there are no standards that ensure ELM compatibility with host tissues. Towards this goal, we designed a 96-well plate-based screening method to streamline ELM growth across culture conditions and determine their compatibility potential *in vitro*. We showed proliferation of three bacterial species encapsulated in hydrogels over time and screened six different cell culture media. We fabricated ELMs in bilayer and monolayer formats and tracked bacterial leakage as a measure of ELM biocontainment. After screening, an appropriate medium was selected that sustained growth of an ELM, and it was used to study cytocompatibility *in vitro*. ELM cytotoxicity on murine fibroblasts and human monocytes was studied by adding ELM supernatants and measuring cell membrane integrity and live/dead staining, respectively, proving ELM cytocompatibility. Our work illustrates a simple setup to streamline the screening of compatible environmental conditions of ELMs with the host.

1. Introduction

Engineered Living Materials (ELMs) lie at the interface between life sciences and materials science. In the biomedical field, these materials have been developed as wearables with biosensing capabilities, and as drug eluting devices with therapeutic and/or regenerative functions [1–7]. When it comes to application, the use of engineered living bacteria in ELMs raises concerns related to biosafety and compatibility with the host [3]. However, the investigation of ELMs *in vitro* lacks standardization and the conditions in which the ELMs perform in most cases are not biocompatible - i.e. they are assessed in bacterial medium [8–10] - or are not specified [11–13]. Duraj-Thatte et al. showed *in vitro* compatibility of ELMs incorporating genetically modified bacteria that produced a mucoadhesive curli protein hydrogel. They tested the cytocompatibility of the ELMs towards Caco-2 cells by performing an MTT assay *in vitro*. They seeded Caco-2 cells on the ELMs but the selected medium was not specified [11]. Liu et al. tested the *in vitro* biocompatibility of their ELM using Caco-2 cells. For the assays, they incubated the ELM without bacteria (i.e., empty hydrogel) in Caco-2 cell culture

medium to then add it to the Caco-2 cells for cytotoxicity tests. Further, bacteria viability in the hydrogels was performed only in LB medium, highlighting the lack of knowledge of ELM viability and performance in host compatible environments [14]. Similarly, Lu et al. designed an ELM encapsulating *Lactococcus lactis* engineered to produce the vascular endothelial growth factor (VEGF) and lactic acid. The characterization of the ELM and ability to produce VEGF and lactic acid were carried out in bacterial M17 medium. However, the angiogenesis assays with HUVECs were performed in DMEM and the immune activation assays using macrophages were carried out in RPMI medium. The ELM ability to produce VEGF and lactic acid in DMEM or RPMI were not shown [8].

The living character of living therapeutic devices requires systematic testing for relevant assessment of their biocompatibility and safety in real application scenarios in contact with the body. However, screening methodologies to systematically assess and optimize ELMs have not been described yet. Screening methods are applied to microorganisms (engineered or not), where the methodology is typically used for the selection of different microorganisms based on the expression of a reporter or a desired phenotype [9,15–17]. For instance, Scanlon et al.

---

described a high-throughput screening method for antibiotic discovery where agarose-in-oil emulsions containing bacteria were used for their screening [9]. Other screening methods make use of hydrogels, for example, Fattahi et al., used a photocleavable hydrogel to screen mutant libraries of bacteria, where desired bacterial phenotypes could be released from the hydrogel by laser ablation for subsequent genotyping [18].

In most cases, systematic studies are required during the design and optimization of ELMs. For example, the selection of engineered bacteria capable of thriving in stressful environments was achieved by Meng et al., where they applied a screening method to select desirable pathway designs and chassis microorganisms, to be applied in future ELMs [19]. Examples of screening methodologies applied to mammalian cells encapsulated in hydrogels exist, usually for tissue engineering and regenerative medicine purposes. However, there are no screening methodologies applied to microorganism-based ELMs. Here, the added hurdle of finding compatible conditions between the microorganism-based ELM and the host requires a high number of co-culture experiments for which parallelized *in vitro* experimental formats and conditions need to be developed. Such experiments need to investigate the behavior of the ELM and the host cells as a function of tissue-dependent composition of the cellular milieu, such as fluctuations in pH, oxygen or nutrient concentration, throughout time.

In this work, we report on important steps to develop predictive assays to test the biocompatibility and safety of ELMs *in vitro*. We describe a simple and versatile methodology to screen ELMs in 96-well plate format across different culture environments. We quantify bacterial proliferation inside the hydrogel, the leakage potential during culture time as a measure of the biocontainment capacity of the material, and the metabolic function of the bacteria inside the hydrogel. We assess the cytotoxicity potential using fibroblasts and monocytes. Our work will help to streamline the development of ELMs by optimizing, early on, the devices compatible with physiological conditions and thus, advancing ELM therapeutic investigations with the host and standardizing practices across ELM developers.

2. Materials and methods

The following reagents were used: LB powder (Lysogeny broth, Art. No. X964.2, Carl Roth GmbH, Germany), MRS powder (Man, Rogosa and Sharpe broth, Art. No. X925.2, Carl Roth GmbH, Germany), BHI powder (Brain heart Infusion, Art. No. X916.2, Carl Roth GmbH, Germany), GlutaMAX (Gibco GmbH, Cat. No. 35050–061, Germany), DMEM (Dulbecco's Modified Eagle Medium) High Glucose (VWR GmbH, Cat. No. SIALD6429, Germany), Roswell Park Memorial Institute (RPMI) 1640 (RPMI (R), Gibco GmbH, Cat. No. 11835030), RPMI 1640 Medium ATCC modification (RPMI supplemented (R_{supp}), Gibco GmbH, Cat. No. 1049101), Penicillin/Streptomycin (Pen/Strep, Gibco GmbH, Cat. No. 15140–122, Germany), Trypsin-EDTA 1x (VWR GmbH, Cat. No. VWRL0154-0100, Germany), Fetal Bovine Serum (FBS) (PAN Biotech GmbH, Germany), vinyl sulfonated - poly (vinyl alcohol) (PVA-VS), LAP (Lithium phenyl-2,4,6-trimethylbenzoylphosphinate, Sigma Aldrich GmbH, Germany), Kanamycin (CAS No. 25389-94-0, Carl Roth GmbH, Germany), Erythromycin (Art. No. X4166.2, Carl Roth GmbH), glycerol (Art. No. 3783.1, Carl Roth GmbH, Germany), 3-(trimethoxysilyl) propyl acrylate (Art. No. 475149, Sigma Aldrich GmbH, Germany), OPI (Art. No. O5003, Sigma Aldrich GmbH, Germany), non-essential amino acids (NEAA, Cat. No.11140–050, Gibco GmbH, Germany), phosphate buffer saline (PBS, without Calcium and Magnesium, VWR GmbH, Germany), DAPI (4′,6-diamidino-2-phenylindole, dihydrochloride, Cas. No. 28718-90-3, Thermo Scientific GmbH, Germany), Tween 20 (Art. No. P1379, Sigma Aldrich GmbH, Germany). All these reagents were used without any modifications.

2.1. Bacteria inoculation

The bacterial strains used in this study were: *Escherichia coli* Nissle 1917 (EcN), *Lactiplantibacillus plantarum* WCFS1(LP), and *Corynebacterium glutamicum* (Cg) constitutively expressing the fluorescent protein, mCherry that is encoded in plasmids suitable for each strain. Plasmid maps for EcN, LP, and EcN are depicted in Figs. S1–3. First, growth medium for each bacterial strain was prepared and sterilized by autoclaving. For EcN, LB was dissolved in MilliQ water (20 g/L) and supplemented with kanamycin (50 μg/mL). For LP, MRS broth was dissolved in MilliQ water (52 g/L) and supplemented with erythromycin (10 μg/mL). For Cg, BHI broth was dissolved in MilliQ water (37 g/L) and supplemented with kanamycin (50 μg/mL). Bacterial (either Cg, EcN or LP) inoculation was carried out by gently scratching the frozen bacterial culture in 20 wt% glycerol (glycerol stocks stored at −80 °C) with a pipette tip. The pipette tip was then added to 5 mL of the growth medium. The bacteria were allowed to grow overnight, and optical density of the cultures were measured at 600 nm (OD600) using a spectrophotometer (Nanodrop 2000, Thermo Scientific GmbH, Germany).

2.2. Bacterial growth in suspension

Bacterial growth in different media was monitored for 15–20 h. After inoculation bacterial cultures were diluted to an OD600 of 0.1 and centrifuged (3 min, 9000 rpm) to obtain a pellet. The bacterial pellets were resuspended in different media. EcN was cultivated in either LB broth or RPMI +10 % FBS (R-10 %). LP was cultivated in MRS Broth, R-10 %, RPMI supplemented +10 % FBS (R_{supp}-10 %) or RPMI supplemented + 20 % FBS (R_{supp}-20 %). Cg was cultivated in either BHI, R-10 %, R_{supp}-10 % or R_{supp}-20 %. Notably, Compared to RPMI® medium, RPMI ATCC Modified (R_{supp}) medium contains HEPES, sodium pyruvate, high glucose content (4.5 g/L) and low sodium bicarbonate (1500 mg/mL).

To assess the possible effect of UV irradiation used for hydrogel polymerization on bacteria growth, 200 μL of bacterial culture or 200 μL of medium (negative control, blank) were transferred to a 96-well plate. The plate was irradiated with the conditions used for photo-crosslinking (3 min 15 s at 6 mW/cm², 365 nm, UV lamp Bio link 365, Labor Technik GmbH, Germany). As controls, bacterial cultures without UV irradiation were used in the same plate. Bacterial growth was monitored for around 20 h by measuring OD600 using a plate reader (TECAN Infinity, Germany). The plate reader was maintained at a different temperature depending on the bacterial strain (37 °C for EcN and LP, 30 °C for Cg). OD600 was read every 20 min at 4 different points in each well. Each measurement cycle started with shaking the plate for 18 min, followed by a rest period of 2 min and the OD600 measurement. Conditions were set in triplicates.

2.3. Bacterial preparation for encapsulation in hydrogels

After growing the bacteria overnight as described above, the cultures were diluted to OD 0.5, centrifuged, and resuspended in the appropriate media to mix with the polymer precursor solutions.

2.4. Hydrogel solutions preparation

PVA-VS (vinyl sulfone modified polyvinyl alcohol, 199–209 kDa, degree of VS-functionalization 0.95–1.34 %) was synthesized as previously reported [7]. A 10 wt% PVA-VS stock solution was prepared by stirring the polymer in MilliQ water at 1050 rpm at a temperature of 90–95 °C during 3–4 h. PVA (130 kDa) was dissolved in a similar way at 10 wt% concentration.

PVA hydrogels were prepared with either a bilayer architecture (i.e., inner layer encapsulating bacteria and outer protective layer preventing bacterial escape) or only inner layer to study effect of biocontainment.

The inner layer was prepared by mixing PVA-VS at a final concentration of 4.75 wt%, PVA at a final concentration of 0.25 wt%, and LAP at a final concentration of 0.5 wt % in the corresponding medium to be tested and the bacterial suspension at final OD600 0.05 in the same medium. The mixture was vortexed for 2 min at 3000 rpm. To prepare the outer protective layer for bilayer hydrogel, LAP at 0.5 wt% final concentration was dissolved in 10 wt % PVA-VS by sonicating for 15 min at room temperature and shaked in an Eppendorf ThermoMixer (40 °C, 1200 rpm) for 15 min. The volumes for each condition tested are specified in Tables S1, S2, and S3. Hydrogels are named X-PVA, X being the bacterial strain used in the inner layer (EcN, LP or Cg). Control gels without bacteria (OD 0) were prepared in both bilayer and inner layer architecture.

2.5. Hydrogel fabrication in μ-plate 96 well 3D

Bilayer hydrogels were prepared in μ-plate 96Well plates (Ibidi, Germany). The 96 wells had a diameter of 5 mm diameter (ca. 70 μL volume) and an internal microwell with 4 mm diameter and 0.8 mm height (ca. 10 μL volume). Prior to hydrogel preparation, the surface of the wells was functionalized with acrylate groups to covalently attach the PVA-VS hydrogel to the surface of the well. For this purpose, 70 μL of absolute ethanol was first added to the wells and the plate was kept on a shaker for 5 min at 300 RPM. After removing the ethanol, 70 μL of a 0.5 % solution of 3-(trimethoxysilyl) propyl acrylate in ethanol were added to the wells and the plate was kept overnight on a shaker at 300 RPM. On the next day, the plate was left under the fume-hood to let the remaining ethanol evaporate. Plates were UV-sterilized for 30 min in a safety laminar flow hood before use. 10 μL of the hydrogel precursor mixture were added to the inner well to obtain the inner layer and polymerized by UV irradiation (365 nm, 6 mW/cm^2) for 45 s using a UV lamp (Bio link 365, Labor Technik GmbH, Germany). Afterwards, 20 μL were added to the well to form the outer protective layer and photo-crosslinked (365 nm, 6 mW/cm^2) for 2 min and 30 s. After polymerization, 50 μL of medium was added. Plates were incubated at 37 °C and 5 % CO_2 for 3 h, after which the medium was exchanged to allow the hydrogels to swell and remove any unreacted LAP unless otherwise noticed (Binder, Germany).

2.6. Quantification of bacterial proliferation in the hydrogels

To quantify bacterial proliferation in the hydrogel, alamarBlue assay (Invitrogen, Germany) was used at different timepoints following manufacturer's instructions. Briefly, medium was exchanged to medium with alamarBlue reagent at different timepoints. 10 % alamarBlue reagent was added to the specific medium to test and hydrogels were incubated at 37 °C (or 30 °C when noted), 5 % CO_2 for 4 h with the reagent. After incubation, 25 μL of the medium was transferred to black 384-well plate and fluorescence was measured using a plate reader (Tecan Biotek, Ex/Em 530/570 nm and 580/610 nm). Samples were measured in triplicates.

2.7. Determination of bacterial leakage from the hydrogels

To test bacteria leakage from the hydrogels after culture, 2 μL of the cultured supernatant were transferred to a 96-well plate and 200 μL of bacterial growth media (MRS Broth supplemented with erythromycin for LP, LB broth supplemented with kanamycin for EcN and BHI medium supplemented with kanamycin for Cg). Positive controls with inoculated bacteria and negative controls with bacterial growth medium were used. These cultures were incubated overnight and the OD600 was measured at the beginning (0 h) and after 24 h or 48 h using a plate reader set at 37 °C (for EcN) or 30 °C (for Cg).

2.8. Fluorescence microscopy

All three bacterial strains expressed mCherry. For live imaging, a Zeiss Celldiscoverer 7 microscope installed with LSM 900 and Airyscan 2 (Zeiss, Germany) was used. Images were taken at 20x/0.95 NA (ZEISS Plan-Apochromat) objective with optovar 1× or 0.5x Tubelens lens. While imaging, the temperature was set at 37 °C. mCherry fluorophore was visualized with a Ex/Em of 561/565–700 nm and Z-stacks of 20 μm were captured at least 50 μm above the bottom of the plate. At least 3 stacks per replicate were taken and 3 replicates per condition were used.

Bacterial colony areas were calculated from stacks of 20 μm at 10X (16–20 images in total). Stacks were projected onto the same plane using the *Z-projection* tool on Fiji (ImageJ v1.54f) and applying the *Max. Intensity* projection. From the projections, masks were obtained using the *threshold* tool (Otsu method, automatic detection) and then individual colonies were selected manually using the *wand* tool. For all timepoints >200 colonies were quantified.

For EcN samples, brightfield images were used at 10X (19 images per timepoint in total). To quantify the colony shape descriptors, masks were obtained first. The flatten calibration tool in Fiji was applied first. Then, the *auto-crop* tool was applied. After that, each image was converted to 8-bit and the *auto-threshold* was applied (Otsu method). Then, the tool *fill holes* was used and colonies on focus were selected with the *magic wand* tool and measured. For each timepoint measured >200 colonies were quantified.

2.9. Cell culture

Fibroblasts (NIH-3T3 cell line, ATCC, mouse, passages 22–27) were used for cytotoxicity assays. Cells were grown in DMEM high glucose and supplemented with 10 % heat inactivated FBS (D-10 %), 1 % GlutaMax, and 1 % Penicillin/Streptomycin. Cell culture was exchanged every other day and cells were passaged (trypsin-EDTA, 3 min at 37 °C, 5 % CO_2) when cell confluency reached around 70 %. Fibroblasts were seeded at a final cell density of 16000 cells/cm^2 in 96-well plates using growth medium (D-10 % + 1 % GlutaMax +1 % Pen/Strep). After 24 h, the culture medium was replaced by supernatants from the bacterial gels (Cg-PVA), which were diluted in R_{supp}-20 % (1:1, V:V). Fibroblasts were incubated with supernatants for 24 h and then, lactate dehydrogenase (LDH) assay and alamarBlue assay were performed.

Monocytes (Mono-mac-6 cell line, ATCC, human, passages between 12 and 15) were used for cytotoxicity assays. Cells were grown in RPMI medium supplemented with 10 % heat inactivated FBS, 1 % GlutaMax, 1 % NEAA, 1 % OPI and 1 % Pen/Strep. Cell culture was changed every other day and cells were diluted to 300,000 cells/mL every 3–4 days (counted as a passage).

Monocytes were seeded at a final cell density of 150,000 cells/mL in 96-well (Greiner Bio-one, Germany) plates using growth medium. After 24 h, the culture medium was replaced by supernatants from the bacterial gels diluted in R_{supp}-20 % (1:1, V:V). Monocytes were incubated with supernatants for 24 h and then, live/dead staining was performed.

2.10. Cytotoxicity assays

To perform the cytotoxicity assays, 50 μL of supernatants from Cg-PVA hydrogels incubated in R_{supp}-20 % and collected on day 1 and day 2 were used and mixed with 50 μL of R_{supp}-20 % medium.

Lactate dehydrogenase (LDH) assay (CytoTox 96® Non-Radioactive, Promega, Germany) was performed to measure cell death following manufacturer's instructions. Briefly, 30 μL of supernatants were transferred to a 96-well plate and mixed with 30 μL of the CytoTox 96® Reagent. The plate was incubated at room temperature (300 RPM, protected from light) for 30 min. After that, the stop solution reagent (30 μL) was added and absorbance at 490 nm was measured using a plate reader. Blanks of each supernatant were used, and lysed cells with 5 μL of 37.5 % Triton X-100 were used as positive control. 5 μL of PBS

was added to samples to keep the same final volume in all the wells.

AlamarBlue assay was performed to determine the number of metabolically active cells. Briefly, 10 % alamarBlue reagent was added to cell culture medium. Cells were incubated with the medium supplemented with alamarBlue reagent for 1.5 h at 37 °C (5 % CO_2). Then, 50 µL of supernatant were transferred to a black bottom 96-well plate. Fluorescence intensities were measured in a plate reader (Ex/Em 570/600 nm). Blanks with only supernatants and positive controls of cells grown in growth medium were included.

2.11. Immunostaining

After performing LDH and alamarBlue assay, fibroblasts were washed twice with PBS and fixed using 4 % PFA (Paraformaldehyde solution) for 30 min at room temperature. After fixation, samples were washed twice with PBS to remove the PFA left. Cells were permeabilized using 0.1 % of triton X-100 in PBS for 5 min at room temperature. Then, cells were washed twice with PBS and blocking buffer (1 % Bovine serum albumin in PBS) was added for 30 min at room temperature. After removing blocking buffer, phalloidin (AlexaFluor 488-Phalloidin, 1:400 dilution, Proteintech, Germany) and DAPI (1:1000 dilution, Invitrogen, Germany) were added and incubated at room temperature for 1 h. Finally, cells were washed five times with wash buffer (0.5 % Tween 20 in PBS) and cells were incubated in PBS while imaging. Zeiss Celldiscoverer 7 microscope installed with LSM 900 and Airyscan 2 (Zeiss, Germany) was used to capture fluorescence images at 20x/0.95 NA (ZEISS Plan-Apochromat) objective with optovar 0.5× Tubelens lens.

2.12. Live/dead staining

Monocytes were stained for viability determination after adding the bacterial gels supernatant overnight. Cells were washed twice with PBS. The live (fluorescein diacetate, 5 mg/mL, Invitrogen, Germany) and dead (propidium iodide, 2 mg/mL, Invitrogen, Germany) staining were added to PBS to make final concentration of 40 µg/mL and 30 µg/mL, respectively. The samples were incubated at room temperature for 15 min. Then, staining was removed, and the samples were washed twice with PBS before imaging. Finally, images were taken immediately using an epifluorescence microscope (Keyence). A minimum of 10 images at 10× magnification were obtained. Quantification of % of live cells was carried out using the 10× magnification images. The % of live cells was calculated as: [number of live cells/total cells] *100.

2.13. Statistical analysis

All experiments were performed in triplicates. Statistical analysis was carried out using GraphPad Prism v9 software. All graphs represent the mean ± standard deviation (SD) unless otherwise noted. The goodness of fit of the data sets was assessed by Normality Shapiro-Wilk test. For comparisons of three groups, normal distributed populations were analyzed via analysis of variance (ANOVA) test followed by a Tukey's *post hoc* test to correct for multiple comparisons. For comparisons of two groups, normal distributed populations were analyzed via parametric *t*-test. For populations of two groups that were not normally distributed, a non-parametric (Mann-Whitney) *t*-test was performed. For comparisons of two groups at different timepoints, populations were analyzed via analysis of variance (two-way ANOVA). Two-way ANOVA was performed by matching timepoint as a factor. A full model was fitted (time (row) effect, condition (column) effect and time/condition (row/column) effect). An equal variability of differences was not assumed and therefore the Geisser-Greenhouse correction was used. Multiple comparisons were performed two ways, first within each condition through time and then comparing conditions per timepoint (column (condition) and row (time) effects). Differences among groups are indicated as follows: *p*-values <0.05 (*), *p*-values <0.01 (**), *p*-values <0.005 (***), *p*-values <0.001 (****), and differences among groups not statistically significant (ns).

3. Results

We investigated ELMs containing three different bacterial strains: 2 gram-positive strains (*Corynebacterium glutamicum* (Cg) and *Lactiplantibacillus plantarum* WCFS1 (LP)) and 1 gram-negative (*Escherichia coli* Nissle 1917 (EcN)). We selected LP and EcN because they are generally recognized as safe (GRAS) in the food industry [20,21], they are natural commensals in humans [22,23], and these probiotic bacteria are highly used in ELMs [8,11,24] and as living biotherapeutic products [25,26]. We selected Cg due to our previous work on a living contact lens prototype [7], where the species *Corynebacterium* represents approximately 80 % of the total eye microbiome [27,28]. For imaging purposes, we used engineered variants of these bacteria strains that expressed mCherry.

We performed initial cytotoxicity assays on murine fibroblasts in LB, BHI or MRS, which are the broths used to culture the selected bacteria strains. The addition of LB, BHI or MRS broths for 24 h to the fibroblasts in culture led to an 8-, 6- and 3-fold decrease in cell viability as measured by alamarBlue assay compared to, for example, RPMI medium supplemented with 10 % FBS (R-10 %) (Fig. 1a). Microscopic observations of cell morphology (Fig. S4) showed a progressive rounding and detachment of the fibroblasts from the well plate when in contact with either LB, MRS or BHI, whereas they presented a spread morphology when cultured in R-10 %, RPMI ATCC modified and supplemented with 10 % FBS (R_{supp}-10 %) and DMEM supplemented with 10 % FBS (D-10 %).

On the other hand, the growth of the bacterial strains (*Escherichia coli* Nissle (EcN), *Lactiplantibacillus* (LP) and *Corynebacterium glutamicum* (Cg)) in suspension in RPMI or DMEM supplemented with 10 % FBS (R-10 %, Rsupp-10 % or D-10 %) showed notable differences between bacterial strain growth and amongst cell culture media assayed (Fig. 1b–e).

EcN grown in R-10 % (Fig. 1b) presented a similar lag phase and slightly lower average growth rate (0.104 hr^{-1}) in the exponential phase compared to LB broth (0.124 hr^{-1}) but the stationary phase in R-10 % was achieved at a lower OD600. LP strain did not grow in R-10 % (Fig. 1c) and, therefore, we investigated growth in RPMI supplemented with high glucose (4.5 g/L), sodium pyruvate, and HEPES with either 10 or 20 % FBS (R_{supp}-10 %, or R_{supp}-20 %). LP grew in both R_{supp}-10 % and R_{supp}-20 %. A longer lag phase compared to MRS broth was observed for both media and the exponential phase was achieved at a lower rate in both cases, R_{supp}-10 % being the slowest (average growth rate of 0.015 hr^{-1}). The stationary phase reached by LP grown in R_{supp}-10 % and R_{supp}-20 % were at a lower bacterial density (OD600 0.41 and 0.37, respectively) compared to MRS broth (0.67).

We also screened different culture conditions in suspension with Cg (Fig. 1d and e). Normally, this bacterium grows at 30 °C, therefore, we started comparing the grow of Cg at 30 °C in their optimal medium (BHI broth) and R-10 %, which supported EcN growth but no LP (Fig. 1d). At 30 °C, the lag phase observed for BHI broth and R-10 % was similar and the growth rate in exponential phase was similar (0.13 hr^{-1}) for both conditions. Differences arose in the stationary phase. On average, Cg growing in R-10 % reached stationary phase sooner compared to BHI broth, resulting on an overall lower final OD600 of 0.65. In BHI broth, Cg continued growing at a slower rate (average growth rate of 0.06 hr^{-1}) compared to the exponential phase and by the end of the experiments Cg had not reached stationary phase. We also tracked the growth of Cg in suspension at 37 °C. At 37 °C, all media screened presented similar growth curves, with a similar lag phase. The exponential phase started approximately at the same time for all the media assayed with slight differences in the growth rate. For example, R_{supp}-10 % and R_{supp}-20 % presented a faster exponential growth (average growth rate of 0.127 hr^{-1} and 0.131 hr^{-1}) compared to BHI (average growth rate of 0.087 hr^{-1}) broth. Stationary phase was reached for all conditions tested, being R-10 % the condition that obtained the lowest number of bacteria
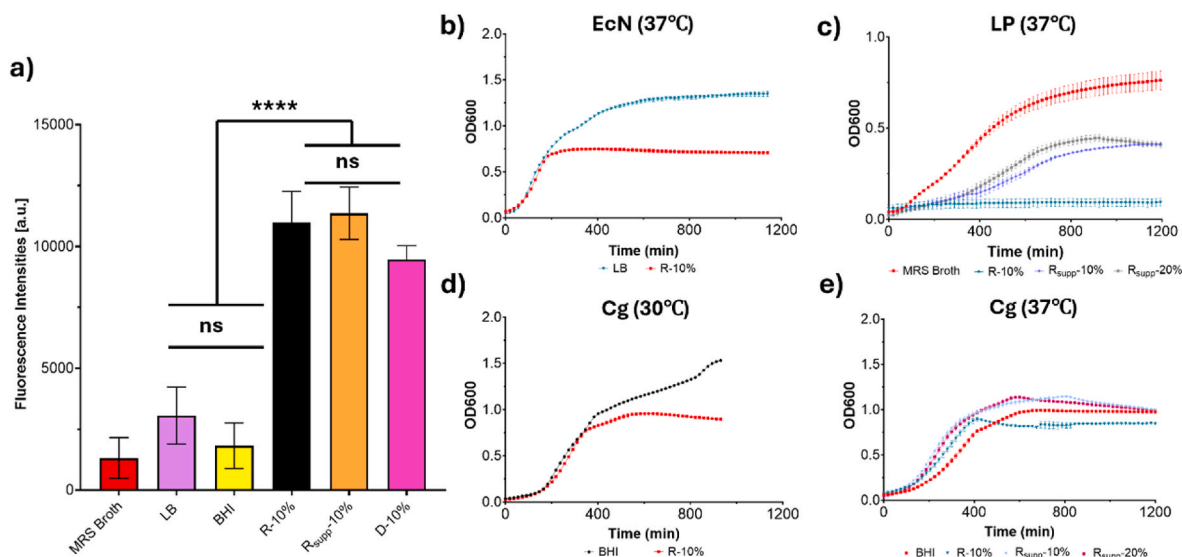
Fig. 1. Mammalian cell culture conditions affect bacterial growth. (a) Viability of fibroblasts in contact with bacterial culture media (MRS Broth, LB, and BHI). R-10 %, R_{supp}-10 % and D-10 % were used as controls; **(b)** Growth curve of EcN in suspension at 37 °C in LB broth (blue line) and RPMI-10 % FBS (R-10 %, red line **(c)** Growth curves of LP in suspension at 37 °C in MRS broth (red line), R-10 % (teal line), R_{supp}-10 % (grey line), R_{supp}-20 % (purple line) **(d)** Growth curve of Cg in suspension at 30 °C in BHI broth (black line), R-10 % (red line) **(e)** Growth curve of Cg in suspension at 37 °C in BHI broth (red line), R-10 % (teal line), R_{supp}-10 % (light blue line), R_{supp}-20 % (purple line). For all plots data is represented as mean ± SD and n = 3 biological replicates.
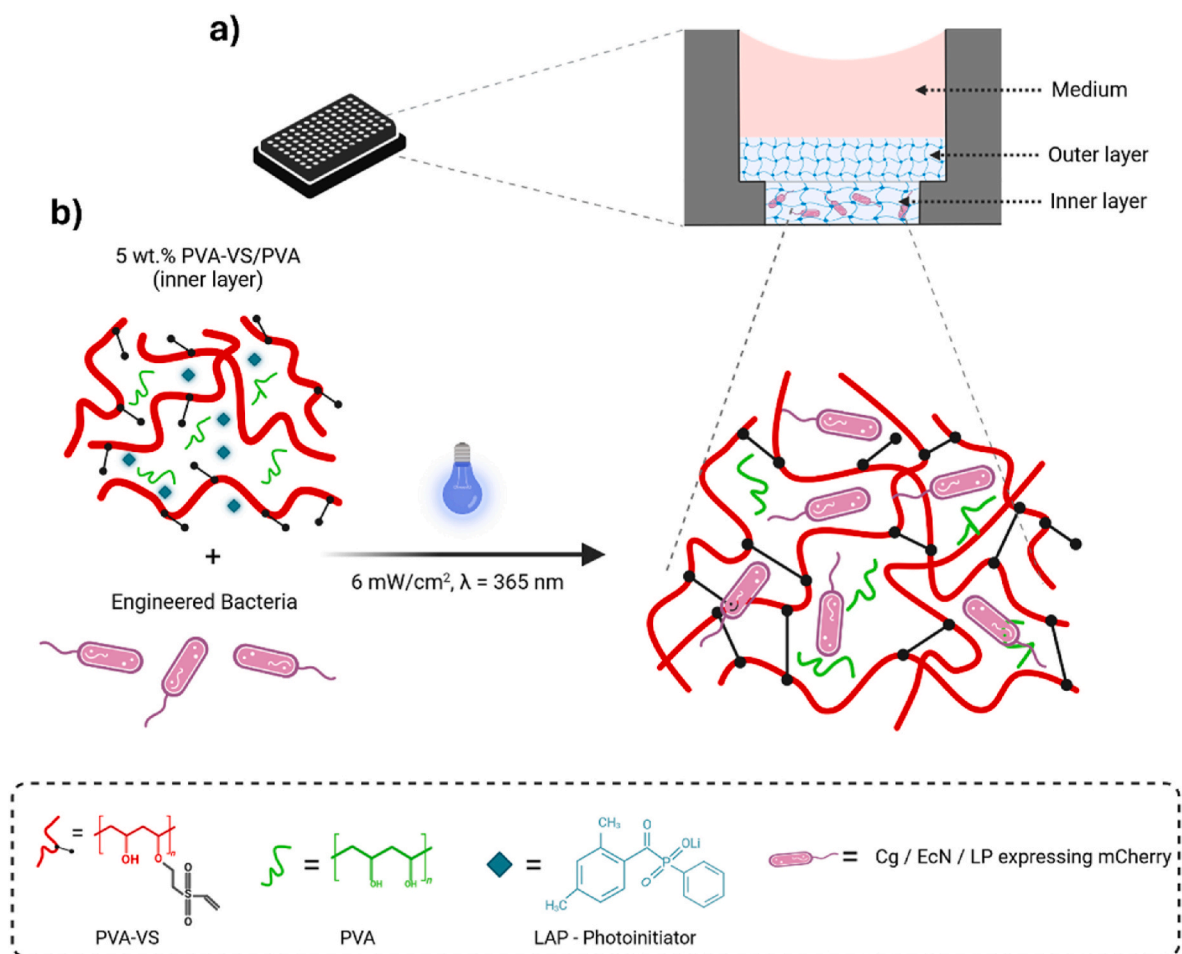

Fig. 2. Composition of the bilayer hydrogel model inside the microwells. (a) PVA-VS/PVA bilayer ELMs fabricated in μ-plate 96 Well. **(b)** Photo crosslinking of bacterial PVA-VS/PVA hydrogels (inner layer) using UV radiation.

(OD600 of 0.89) at the end of the experiment.

The development of a more systematic screening method of the behavior of ELMs in different environments was motivated by i) the differences observed in bacterial growth in suspension in different media and ii) the viability decay observed in fibroblasts cultured in LB, MRS and BHI broths. This method aims to identify suitable conditions for co-culturing mammalian cells and bacteria-based ELMs.

We selected PVA-VS/PVA mixtures as hydrogel matrix for our ELMs since these have been successfully used by us and others in previous reports [7,8,29,30]. Bilayer hydrogels were prepared in 96well-plates with a well-in-well architecture (Fig. 2a). The bilayer hydrogels had an inner layer containing the bacteria and composed of 4.75 wt% PVA-VS and 0.25 wt% PVA (before swelling) and bacteria at OD0.05. The outer layer, with a protective function, did not contain bacteria and was composed of 10 wt% PVA-VS (before swelling) (Fig. 2b). These PVA/PVA-VS concentrations were selected considering our results in previous work with PVA-VS/PVA hydrogels for ELMs [7].

Prior to encapsulation in the hydrogels, we studied the effect of UV irradiation used to polymerize the hydrogels on bacterial viability in suspension cultures. No differences in bacterial growth were observed between LB and LB_UV irradiated, or R-10 % and R-10 %_UV irradiated (Figs. 1b and S5a).

We studied viability and growth of EcN within the PVA hydrogels (EcN-PVA gels) in R-10 % medium (Fig. 3). We used alamarBlue assay to investigate EcN proliferation, as a measure of their metabolic activity. As shown in Fig. 3a, bacteria grew inside the hydrogels from day 0 to day 1. We also tracked their growth via imaging as an independent measure of bacterial proliferation. Fig. 3b shows whole well images of the bacterial hydrogels with increasing culture time, where growing colonies

can be observed. From these images, we quantified colony size and EcN formed colonies on day 1 that were bigger in size on day 2 (Fig. 3c). EcN-PVA bilayer gels cultured in R-10 % presented bigger and more sparse colonies compared to the LB broth control (Fig. S6). As a measure of biocontainment, we tracked the occurrence of bacterial leakage from these ELMs by taking a small volume of the supernatant and using it to inoculate a suspension culture. Of all the EcN-PVA bilayer gels fabricated, 5 % of the gels leaked on day 2 (Fig. 3d).

To compare the functionality of the bacteria inside the different media, we tested protein production by imaging the fluorescence coming from the expression of mCherry (Fig. 3e). High magnification images of the colonies showed that even though there is variability amongst bacteria, on average the expression of mCherry is distributed across the area of the colonies imaged.

Next, we encapsulated a Lactobacillus strain (LP) (Fig. 4) and screened different cell culture media. Prior to encapsulation, we studied the effect of UV irradiation on LP growth in suspension (Fig. S5). UV irradiation for LP culture in MRS broth did not change its growth profile over time. Notably, LP did not grow in R-10 %, irrespective of UV irradiation. UV treatment did not affect LP growth in R_{supp}-10 % or R_{supp}-20 %.

Then, we encapsulated LP in PVA bilayer gels and tracked their growth in R_{supp}-10 % and MRS broth, which allowed the growth of LP in suspension (Fig. 1c, Fig. S7). The proliferation of LP in LP-PVA bilayer gels was studied via alamarBlue assay (Fig. S7a). No growth was observed in Rsupp-10 % for up to 2 weeks. LP-PVA bilayer gels incubated in MRS broth (Fig. S7b) presented high fluorescence values on day 1 but a steep decrease in fluorescence by day 2, measured by alamarBlue. The observations from brightfield or fluorescence images
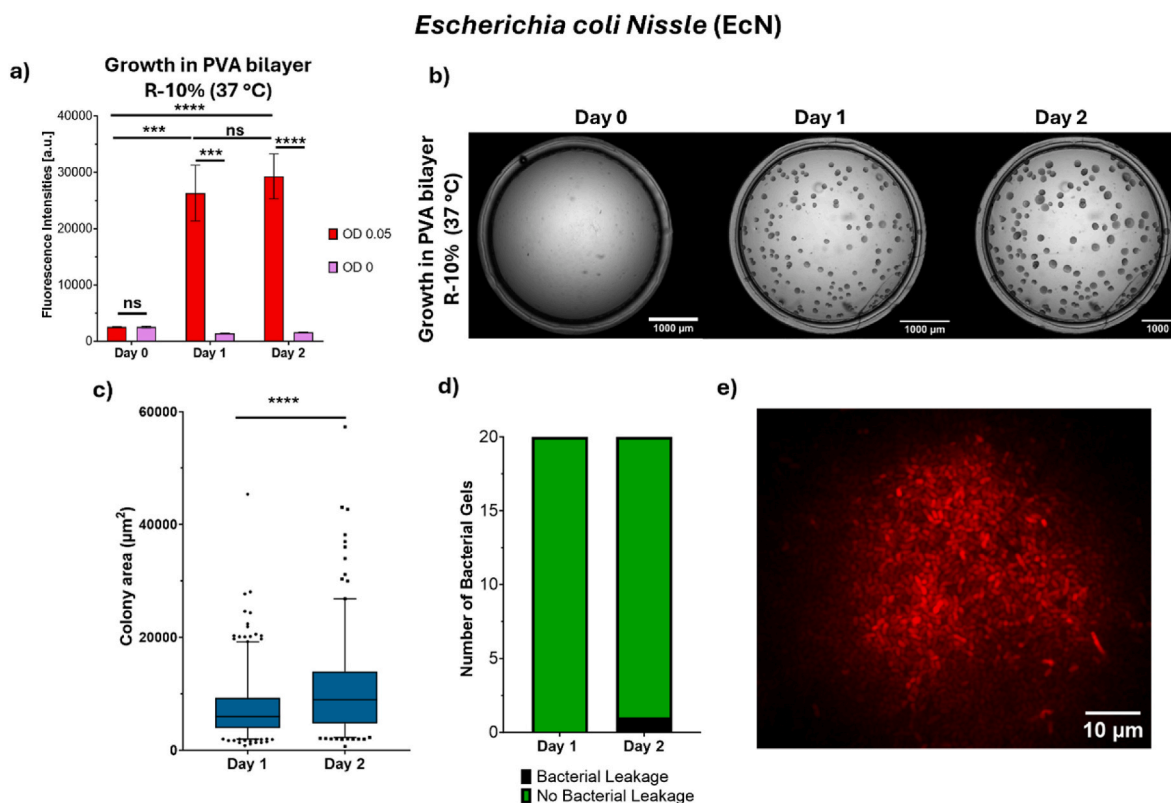

Fig. 3. EcN encapsulated in PVA bilayer hydrogels grow in R-10 % medium at 37°C.
Bacterial hydrogels were fabricated by encapsulating a final OD600 of 0.05 and an empty hydrogel control (OD 0) was used. **(a)** Proliferation (manual gain 65, alamarBlue assay) of EcN encapsulated in PVA hydrogels (EcN-PVA gels) and incubated in R-10 % at 37 °C (n ≥ 3 biological replicates, mean ± SD). **(b)** Bright field images of the whole wells containing EcN-PVA gels (scale bar: 1000 μm). **(c)** Colony area quantification (μm^2) from EcN-PVA (The line within the box signifies the median value, and the whiskers denote the range between the 5th and 95th percentiles, with outliers depicted as dots positioned above or below the whiskers) **(d)** Quantification of leakage from EcN-PVA gels **(e)** Representative high magnification image of a single colony (Scale bar: 10 μm). Differences among groups are indicated as follows: p-values <0.05 (*), p-values <0.01 (**), p-values <0.005 (***), p-values <0.001 (****), ns = not significant.
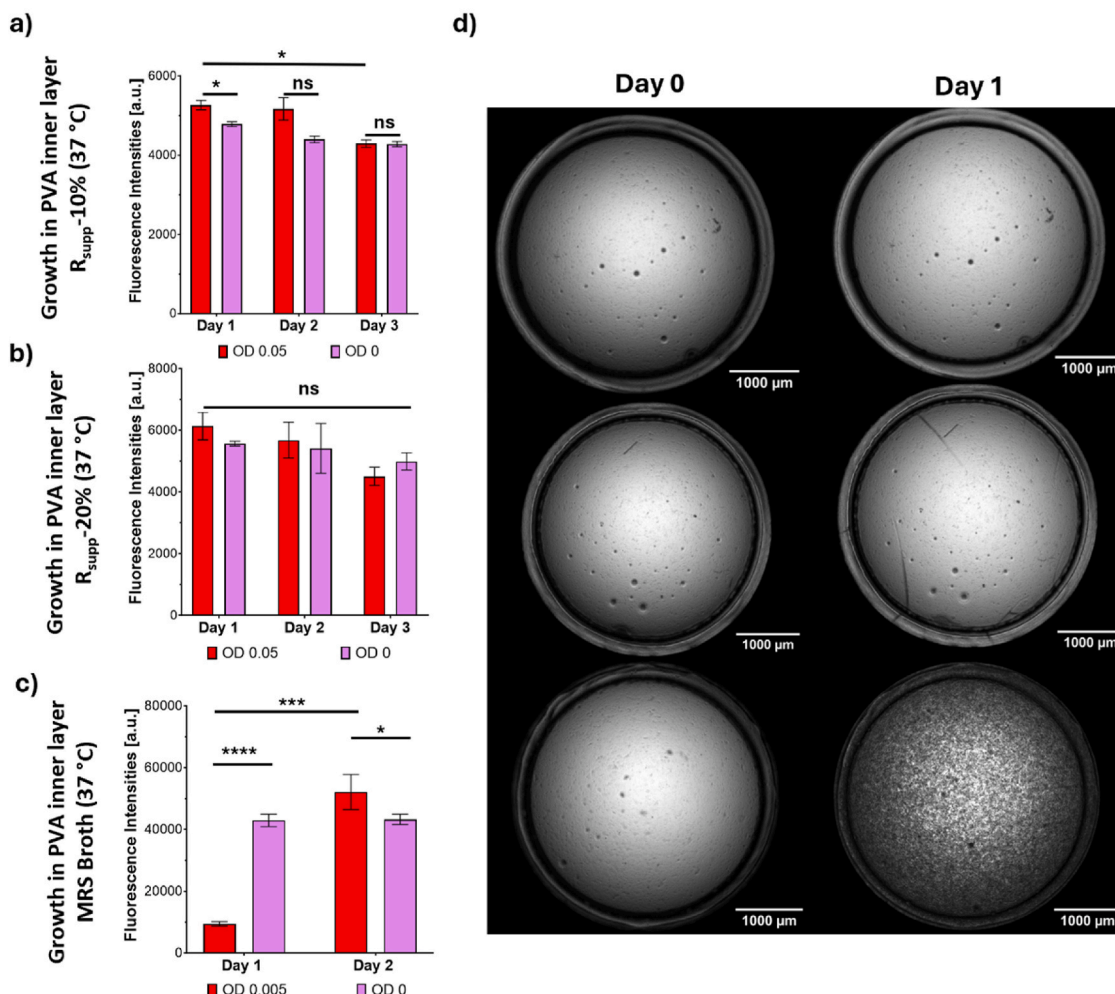
Lactiplantibacillus (LP)

Fig. 4. LP encapsulated in PVA inner layer hydrogels only grow in MRS broth at 37 °C.
Proliferation (manual gain 80, alamarBlue assay) of LP-PVA inner layer gels in **(a)** R_{supp}-10 % **(b)** R_{supp}-20 % and **(c)** MRS Broth at 37 °C. (n = 3 biological replicates, mean ± SD) (d) Bright field images of inner layer gels encapsulating LP mCherry in R_{supp}-10, R_{supp}-20 %, and MRS Broth on day 0 and day 1, respectively. Scale bars: 1000 μm. Differences among groups are indicated as follows: p-values <0.05 (*), p-values <0.01 (**), p-values <0.005 (***), p-values <0.001 (****), ns = not significant.

showed a different outcome (Fig. S7c): here colonies were observed by day 1. Colony areas increased from day 1 to day 2 (Fig. S7d) and LP were seen expressing mCherry homogenously on average and across the colonies, although some differences in fluorescence intensity are observed amongst bacteria (Fig. S7e). It is noteworthy that colony size for this strain was approximately 50-fold smaller compared to EcN grown in R-10 %.

To investigate whether the presence of the outer hydrogel layer was hindering growth for LP in R_{supp} media, we tracked proliferation of LP in PVA inner layer gels, without the outer layer (Fig. 4). We incubated the gels in R_{supp}-10 %, R_{supp}-20 % and MRS broth. Data obtained from the alamarBlue assay showed similar results to bilayer encapsulation for R_{supp}-10 % and R_{supp}-20 % (Fig. 4a and b). MRS medium showed similar results as well, with a high decrease in fluorescence by day 2 (Fig. 4c). From the brightfield images (Fig. 4d), we confirmed that LP did not grow in the inner hydrogel layer cultured in R_{supp}-10 % and R_{supp}-20 %, whereas in MRS the bacteria formed colonies similarly to what was observed in bilayer hydrogels.

We next studied the growth of Cg in PVA gels. Prior to that, we confirmed that UV irradiation did not affect Cg growth in suspension (Fig. S5c). Then we investigated Cg-PVA bilayer gels incubated in R-10

% at 37 °C using alamarBlue assay (Fig. S8a). Bacteria did not grow in these conditions for up to 3 weeks. They also did not grow at 30 °C in R_{supp}-10 %, R_{supp}-20 % and BHI broth (Figs. S8b–d). We then compared the proliferation of Cg-PVA in hydrogels that only contained the inner layer at 30 °C in BHI broth and R_{supp}-20 % (Fig. 5a and b). We observed an increase in proliferation via AlamarBlue assay on day 1 for both BHI broth and R_{supp}-20 %. The brightfield images (Fig. 5c) showed proliferation of Cg in the inner layer gels in R_{supp}-20 % with colony formation, which was not observed in BHI broth at the same timepoints. Cg also did not grow when encapsulated in the outer layer (Fig. S9, which could be due to the denser network of the outer layer compared to the inner layer, where Cg did grow in R_{supp}-20 %.

Then, we studied the growth of Cg-PVA inner layer gels at 37 °C (Fig. 5d–i). Fig. 5d shows that Cg-PVA inner layer gels at 37 °C incubated in BHI grew during the first 24 h. When incubating Cg-PVA inner layer gels in R_{supp}-20 % at 37 °C, we observed rapid growth on day 1. This growth was maintained after day 2 (Fig. 5e). From these constructs, we did not observe any leakage of bacteria up to day 2 (Fig. 5g). Cg-PVA inner layer gels incubated in R_{supp}-20 % were also characterized via brightfield images and fluorescence microscopy (Fig. 5f–i). On day 1, Cg were forming colonies and the number of colonies per field of view

Corynebacterium glutamicum (Cg)
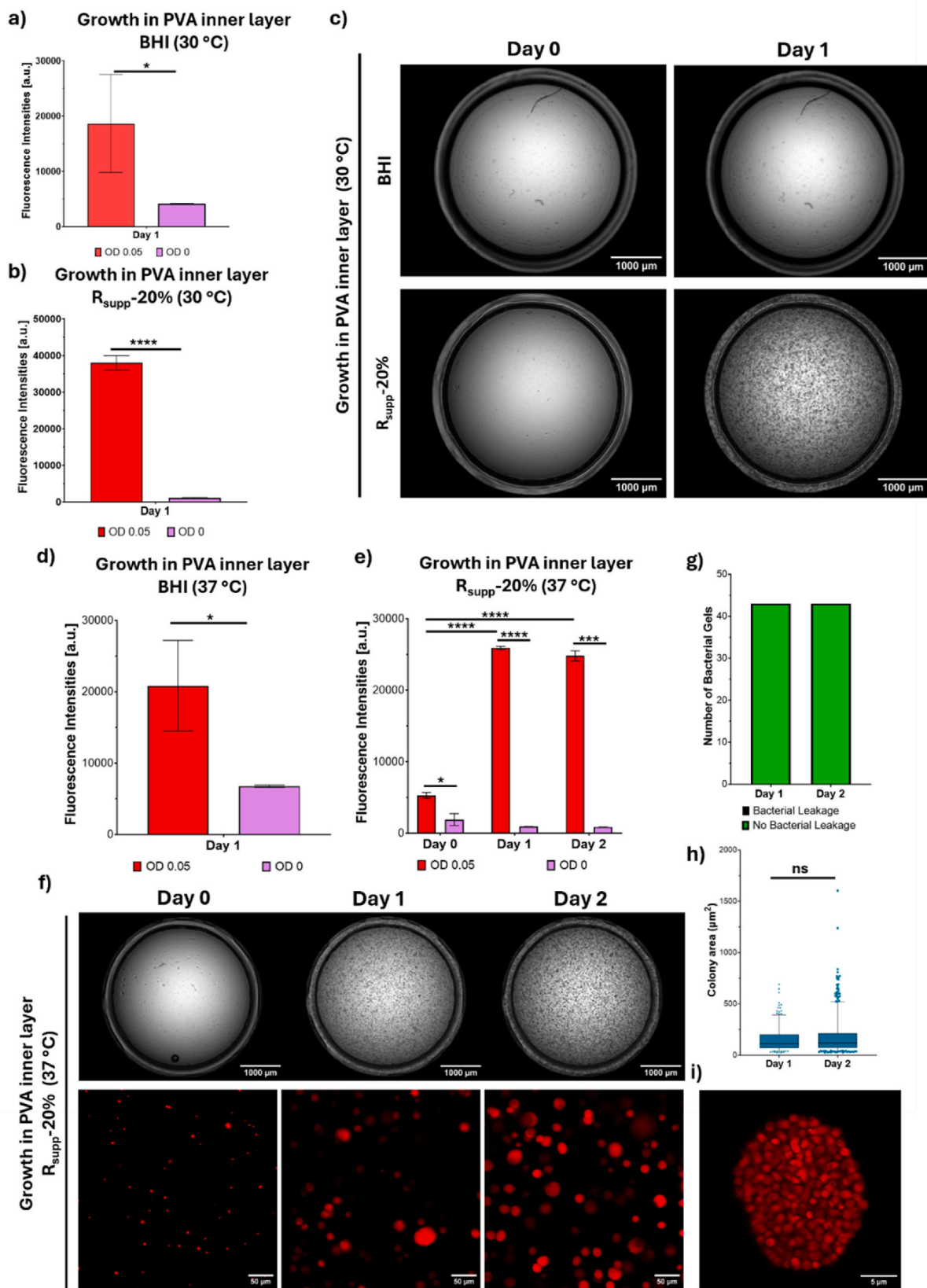
(caption on next page)

Fig. 5. Cg encapsulated in PVA inner layer hydrogels grow in R$_{supp}$-20 % at 37°C.
(a) Proliferation (manual gain 65, alamarBlue assay) of Cg-PVA inner layer gels in BHI broth at 30 °C, **(b)** Proliferation of (manual gain 65, alamarBlue assay) Cg-PVA inner layer gels in R$_{supp}$-20 % at 30 °C (mean ± SD). Differences among groups are indicated as follows: p-values <0.05 (*), p-values <0.01 (**), p-values <0.005 (***), p-values <0.001 (****). **(c)** Representative bright field images of Cg-PVA inner layer gels (scale bar: 1000 μm). **(d)** Proliferation of (manual gain 65, alamarBlue assay) Cg-PVA inner layer gels in BHI broth at 37 °C, **(e)** Proliferation of (manual gain 65, alamarBlue assay) Cg-PVA inner layer gels in R$_{supp}$-20 % at 37 °C, **(f)** Representative bright field images and Z-stack images (Z = 20 μm, Sum Intensities) of Cg-PVA inner layer gels (scale bars: 1000 μm and 50 μm, respectively). **(g)** Quantification of leakage from Cg-PVA inner layer gels in R$_{supp}$-20 % at 37° **(h)** Colony area quantification from the images (The line within the box signifies the median value, and the whiskers denote the range between the 5th and 95th percentiles, with outliers depicted as dots positioned above or below the whiskers). **(i)** Representative high magnification image of a single colony (Scale bar: 5 μm). Differences among groups are indicated as follows: p-values <0.05 (*), p-values <0.01 (**), p-values <0.005 (***), p-values <0.001 (****), ns = not significant.

increased on day 2 (Fig. 5f). Quantification of colony area showed that colonies formed on day 1 and 2 presented a similar average area (Fig. 5h). High-magnification images showed that the production of mCherry was uniform across the section of the colonies, even though there can be seen some differences in fluorescence intensity among bacteria (Fig. 5i). The uniformity of fluorescence observed in the colony could be due to small oxygen gradients available at the time and length-scales of these experiments, as it is known that mCherry requires oxygen for its activation.

For biocompatibility assessment, we performed studies with supernatants collected from Cg-PVA gels (Fig. 6a) which we used in previous studies [7]. Cg-PVA gels were fabricated in inner layer hydrogels using the 96-well plate set up. First, we studied the viability of fibroblasts using LDH assay (Fig. 6b). From this assay we quantified that only 10 %

of the cells had cell membrane disruption after addition of supernatants for 24 h. Alamarblue assay showed a lower reduction of the tetrazolium salt for cells that were in contact with bacterial supernatants (Cg-PVA) compared to cells in our controls (Fig. 6c). Fluorescence intensities were similar to controls with pH adjusted to 5.5 (Fig. 6c), which was the pH measured for the bacterial supernatants. Immunostaining revealed no appreciable differences in cell morphology (Fig. 6d, Fig. S10). We also carried out viability assays using monocytes via Live/Dead staining after addition of Cg-PVA supernatants (Fig. 6e, f, Fig. S10). Viability was similar for both bacterial supernatants and the empty hydrogel controls on day 1. Results showed that approximately 30 % of cells remained viable on average, similar to the control condition with adjusted pH to 5.5 and significantly lower than the positive control.
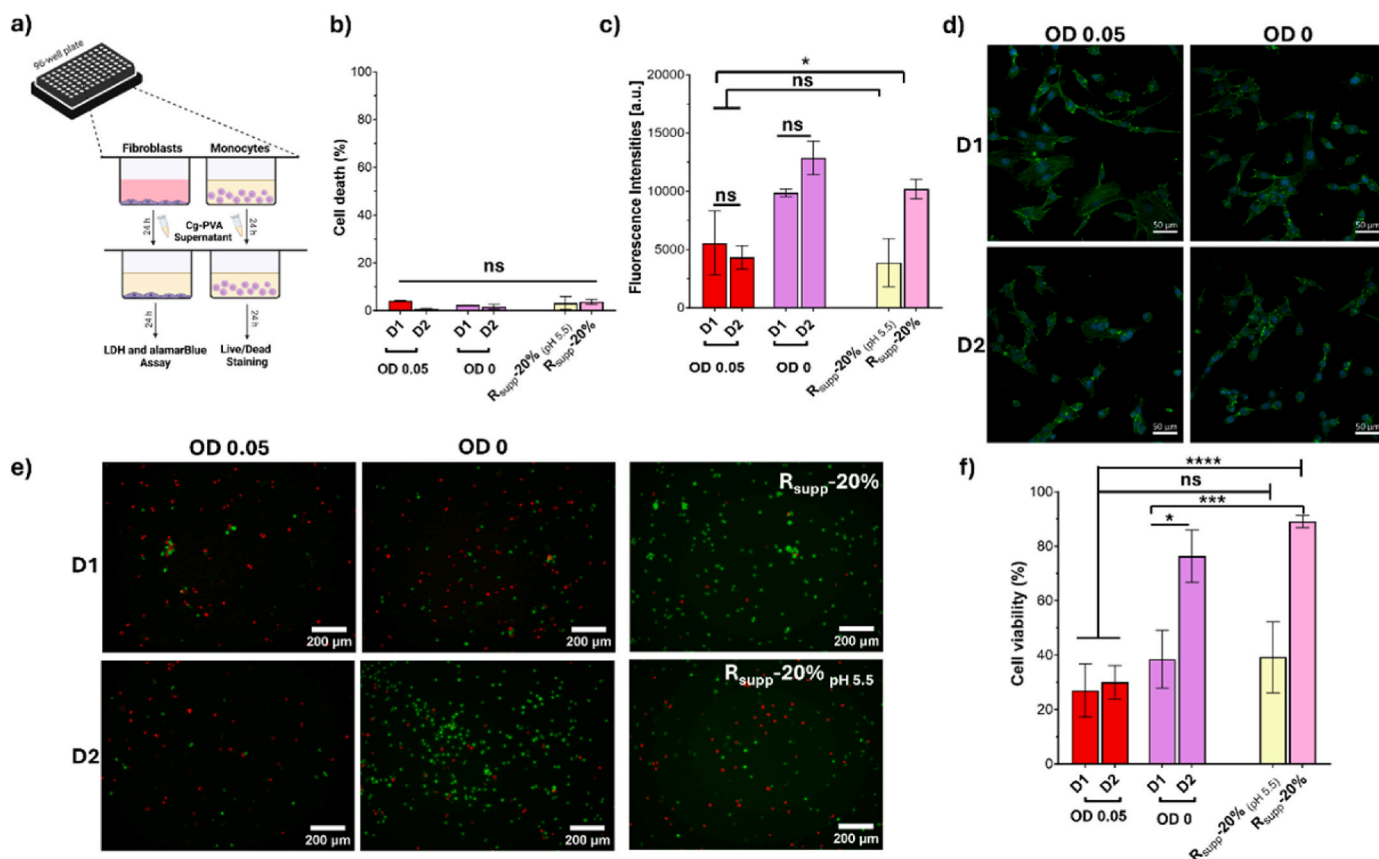

Fig. 6. Biocompatibility studies on Cg-PVA hydrogels. (a) Representation of the procedures carried out to assess cytocompatibility of Cg-PVA supernatants. **(b)** Lactate dehydrogenase assay (LDH) on fibroblasts (NIH-3T3) with supernatants from day 1 and 2 of Cg-PVA gels OD 0.05 and OD 0. R$_{supp}$-20 % and R$_{supp}$-20 % with pH adjusted to pH 5.5 were used as controls, **(c)** fluorescence intensities measured during alamarBlue assay experiments on fibroblasts in contact with supernatants from day 1 and 2 of Cg-PVA gels OD 0.05 and OD 0. R$_{supp}$-20 % and R$_{supp}$-20 % with pH adjusted to pH 5.5 were used as controls. **(d)** Representative images of fibroblast morphologies after addition of supernatants from Cg-PVA gels OD 0.05 and OD 0 at days 1 and 2 (green: cytoskeleton, blue: nucleus, scale bar: 50 μm). **(e)** Representative images of live/dead staining of monocyte cells (mono-mac 6) in contact with supernatants of Cg-PVA gels OD 0.05 and OD 0 on days 1 and 2 where green depicts alive cells and red dead cells. Live/dead images from controls (R$_{supp}$-20 % and R$_{supp}$-20 % with pH adjusted to 5.5) are also shown. **(f)** Quantification of percentage of live cells was carried out from the images (mean ± SD, n ≥ 9, all statistically different comparisons are shown, all other comparisons are ns). Differences among groups are indicated as follows: p-values <0.05 (*), p-values <0.01 (**), p-values <0.005 (***), p-values <0.001 (****).

4. Discussion

Understanding how environmental and culture conditions affect ELMs is critical for their functionality and performance. For microorganism-based ELMs, the specific requirements of each microorganism need to be optimized independently [31]. For ELMs interfacing mammalian cells is even more critical, making necessary screening strategies that couple assays that track maintenance of ELMs while retaining compatibility with mammalian cells.

There are no screening strategies developed specifically for microorganism-based ELMs, which need systematic optimization. ELMs applied to the host present the added obstacle of host compatibility (Fig. 1). The use of bacterial medium in ELM development has been raised as a biocompatibility concern [10]. Some authors circumvent this problem by assessing cytotoxicity *in vitro* with empty hydrogels (i.e., without microorganisms) [14,32], which could be due to problems finding compatible environments for supporting microorganisms and host cells altogether. As we show in Figs. 1c and 4, some microorganisms grow in one medium in suspension but not in the same medium encapsulated in a hydrogel (e.g. LP in R$_{supp}$-20 %). Other authors do not specify in which medium they performed the assays for the ELM-host co-cultures [12,13] or they perform the co-cultures in typical mammalian cell culture media without assessing the viability of the ELM in these environments [33,34].

To improve standardization, we developed an ELM microarray in structured 96-well plates, to retrieve key information about ELM functionality together with host compatibility in an easy, robust way. The well-in-well architecture of the structured plates is well-suited for ELM fabrication, which allowed us to assay bilayer and single layer formats. These formats are typically used for ELMs to enhance the biocontainment properties of the material [35,36]. Further, we chose readouts that could be carried out in parallel using the 96-well plates and therefore, our screening methodology could track bacterial proliferation with alamarBlue and at the same time obtain brightfield images of the whole well and confocal images. Further, by using the supernatants we could measure the occurrence of bacterial leakage as a measure of ELM biocontainment and test their compatibility with mammalian cells. From the images obtained, we were able to measure colony area as another parameter of bacterial growth. This methodology streamlines ELM proliferation investigation in different environmental conditions. In particular, biocontainment strategies are highly sought in the ELM community as they are regarded as a critical safety parameter.

We started investigating EcN as it has been already reported to grow forming colonies in Pluronic-based ELMs when cultivated in RPMI medium [24]. Taking this into consideration, RPMI was chosen for initial experiments. To cope up with the nutritional requirements of mammalian cells, RPMI medium was supplemented with 10 % FBS. Bacterial growth in R-10 % (Fig. 3) was noticeably lower compared to LB (control, Fig. S6), which could be attributed to the higher amino acid to carbohydrate ratio present in RPMI as explained by Wijesinghe et al. [37]. These results were also in line with results from Rebai et al., where growth curves of EcN in RPMI had overall lower OD600 compared to LB broth [38]. It is noteworthy that UV irradiation did not significantly affect EcN growth in R-10 % or LB medium in suspension, as well as observed for LP and Cg (Fig. S5). These findings were consistent with results reported by Li et al. for chemokine CXCL-12 secreting *Lactococcus lactis* [32]. Hydrogels should allow nutrient supply and gas exchange, so the encapsulated bacteria stay metabolically active and proliferating, as demonstrated by others [8,29,36,39]. This was also the case for our ELMs as seen by an increase in fluorescence intensities of EcN-PVA bilayer gels in our proliferation studies (Fig. 3). The colonies formed by EcN within our ELMs increased in size from day 1 to day 2 (Fig. 3). These results agreed with the study from Liu et al. where EcN formed colonies in PVA-based magnetic ELMs [14] and from Riedel et al., where EcN viability in PVA gels was maintained for up to 3 weeks [29]. Interestingly, the fluorescence intensities plateaued by day 2 and in

contrast, the colonies grew from day 1 to day 2 (Fig. 3). This can be explained by differences in metabolic activity of tightly packed colonies, nutrient competitive environment, and diffusion barriers. These stressed conditions could have induced microbial dormancy as discussed by Wood et al. [40,41]. On the other hand, if bacteria had consumed all alamarBlue reagent available to them, then this could have also contributed to the observed plateau in alamarBlue assay.

The nutrient content and its concentration in medium affect the colony sizes [42]. EcN colonies were considerably larger in R-10 % medium compared to LB medium (Fig. 3 and S6), which can be ascribed to its nutrient richness. In a similar study, *Phascolarctobacterium* grown with and without succinate on agar plates resulted in macro and micro colonies, respectively [43]. Nutrient and colony size correlations have been also observed in *Escherichia Coli*, forming smaller colonies when increasing glucose concentration in M63 medium [44]. In addition, Chacón et al. reported that *Salmonella enterica* colony sizes increase when changing the energy source to LB from acetate [45].

After successfully growing EcN-PVA in R-10 % medium, we tried the same medium for LP-PVA bilayer gels with no success. The lack of growth in LP can be attributed to its 10-fold lower glucose concentration (2.0 g/L) compared to MRS broth. Interestingly, LP grew in R$_{supp}$-10 % (R-10 % medium supplemented with extra glucose, HEPES buffer and sodium pyruvate) in suspension (Fig. 1). LP-PVA bilayer gels did not proliferate for 14 days in the same medium (Fig. S7). The alamarBlue assay has been previously reported to determine metabolic activity of LP in liquid culture [46] and also in confinement [47]. However, we had some discrepancies in our results. In agreement with Jun et al., the color of alamarBlue reagent and MRS broth mixture changed from blue to pale yellow. This can be explained by the acidic environment caused by the lactic acid produced by LP, which in turn, reacts with alamarBlue reagent [48]. To increase medium diffusion, we decided to eliminate the outer protecting layer. Additionally, we cultivated LP-PVA inner layer gels in a richer medium (R$_{supp}$-20 %). However, that did not increase bacterial growth, suggesting that LP might have other nutritional requirements. In other ELMs containing *Lactobacillus* species (different strains), medium used for *in vitro* co-culture with mammalian cells was not specified [8,49]. In another example, *Lactococcus lactis* was grown in biofilm form and maintained viable in DMEM supplemented with tetracycline, sulfamethoxazole, erythromycin and without FBS [50]. These observations showcase the importance of a screening methodology like the one presented here, as each microorganism has its particular requirements. Further optimization of the material composition might be required, or other nutritional requirements need to be included in the cell culture medium to achieve compatible conditions for LP growth in the PVA hydrogels used in this study.

For the third bacterial strain, Cg, the optimal medium and temperature for growth is 30°C and BHI medium, respectively [51]. We opted for R-10 % medium due to its similar glucose concentration (2.0 g/L) to BHI medium. Further, as the planned application for these ELMs are at physiological conditions, we monitored their growth at 37 °C in suspension. We found that these bacteria had overall slower growth at 37 °C compared to 30 °C (Fig. 1). We tried to grow Cg-PVA bilayer gels at 30 °C and with supplemented media (R$_{supp}$-10 % and R$_{supp}$-20 %) but observed no bacterial growth (Fig. S8). However, the lack of growth observed for Cg-PVA gels in BHI medium at 30 °C suggested that the 3D confinement environment and the possible lower oxygen diffusion through the bilayer gel format might have hindered proliferation. For example, Shyamkumar et al. observed lower glutamic acid production by Cg encapsulated in alginate constructs when increasing alginate concentration [52]. Cg is a facultative anaerobe and presents preferential growth in aerobic conditions, whereas it halts the growth in oxygen depriving conditions, although it can continue to survive in the presence of glucose [53]. Further, as measured previously by us 10 wt% PVA-VS (our outer layer) has an oxygen permeability of 50 Dk [7] compared to the 80 Dk of water [54]. Considering this, we decided to eliminate the outer protecting layer to aid the oxygen diffusion through the Cg-PVA

gels. We observed Cg growth forming colonies in Cg-PVA gels at both 30 °C and 37 °C (Fig. 5). Interestingly, no colonies formed for Cg-PVA gels cultivated in BHI by day 1, which again stressed the critical role played by the chosen growth medium on growth behavior in confinement. Further, encapsulating Cg in the outer layer resulted in no growth compared to the inner layer, where the only difference between both was the polymer concentration (5 wt% for inner layer and 10 wt% for outer layer) (Fig. S9). This stresses the influence of the material in bacteria growth. In this case, the lack of growth in a denser hydrogel network could hinder oxygen and nutrient diffusion enough to prevent Cg proliferation.

In vitro biocompatibility was assessed for Cg-PVA inner layer gel supernatants on fibroblasts and monocytes. Fibroblasts exposed to the Cg-PVA supernatants showed a decrease in fluorescence measured in alamarBlue assay (Fig. 6c), which differed from values obtained for fibroblasts exposed to supernatants from empty gels (OD 0) and negative control (R_{supp}-20 %). Under oxygen depriving conditions, these bacteria produce succinic acid along with other acids making the ELM supernatant acidic [55], which could explain why the fluorescence values obtained for fibroblasts in contact with Cg-PVA supernatants were similar to a control medium with pH adjusted to 5.5 (acidic control). Similar results were obtained for viability studies performed on monocytes after addition of Cg-PVA supernatants (Fig. 6e, f). Likewise, while co-cultivating human mesenchymal stem cells (hMSCs) and ELMs incorporating engineered *Lactococcus lactis*, Hay et al. obtained low *in vitro* cell viability of hMSCs and attributed it to medium acidification due to accumulation of lactic acid [56]. This stresses the idea that the dynamic nature of ELMs requires *in vitro* platforms that can systematically assess different parameters with time. Our 96-well plate-based screening method can tackle many of these parameters with the limitation that it only allows for relatively small volumes (70 μL capacity) and therefore, glucose consumption, waste accumulation and acidification of media might occur at a higher pace. Possible solutions could be included, such as better buffering systems or a more continuous media exchange during culture, which should be addressed independently for each ELM.

5. Conclusions

In conclusion, this work presents a methodology specifically designed to systematically screen ELM culture conditions to assess the effect of environmental settings on ELM-host interactions *in vitro*. This setup allowed the parallel investigation of ELM proliferation in 20+ different microenvironmental conditions. We were able to assess bacteria proliferation in ELMs with three different bacterial species (EcN, LP and Cg) across 6 different cell culture media. We screened ELMs in bilayer and inner layer formats and measured the probability of bacterial leakage from the ELMs. We tracked colony growth via imaging with both light and fluorescence microscopies and were able to obtain high-magnification images with single bacteria resolution. Shape descriptors of bacterial colonies such as colony area were also implemented. *Corynebacterium* has appeared to be a suitable species for ELMs with application to the eye as it is one of the main species in the eye microbiome. We took supernatants from Cg-PVA inner layer gels that grew in R_{supp}-20 % and studied cell biocompatibility. We selected a stromal, adherent murine cell line (NIH-3T3) and a non-adherent, immune, human cell line (mono-mac 6), and investigated their compatibility with our ELMs. Using this setup, we were able to find suitable culture media for two out of three bacterial strains investigated, highlighting the complexity of finding suitable co-culture conditions for all bacteria applicable in ELM research. We also performed initial biocompatibility studies in co-culture with mammalian cells. We did not showcase this screening technology at the high-throughput scale – i.e., with 96 conditions at once – however, we believe that it has potential to be implemented at this scale, if required. All in all, our setup has the potential to streamline research of ELMs in the biomedical field, helping in their translation from bench to bedside.

CRediT authorship contribution statement

Krupansh Desai: Writing – review & editing, Writing – original draft, Methodology, Investigation, Formal analysis, Data curation, Conceptualization. **Shrikrishnan Sankaran:** Writing – review & editing. **Aránzazu del Campo:** Writing – review & editing. **Sara Trujillo:** Writing – review & editing, Writing – original draft, Supervision, Resources, Project administration, Methodology, Investigation, Funding acquisition, Data curation, Conceptualization.

Declaration of competing interest

The authors declare that they have no known competing financial interests or personal relationships that could have appeared to influence the work reported in this paper.

Appendix A. Supplementary data

Supplementary data to this article can be found online at https://doi.org/10.1016/j.mtbio.2024.101437.

Data availability

Data is openly available at: DOI 10.5281/zenodo.13353844

References

[1] P.Q. Nguyen, N.D. Courchesne, A. Duraj-Thatte, P. Praveschotinunt, N.S. Joshi, Engineered living materials: prospects and challenges for using biological systems to direct the assembly of smart materials, Adv. Mater. 30 (19) (2018) e1704847.

[2] L.K. Rivera-Tarazona, Z.T. Campbell, T.H. Ware, Stimuli-responsive engineered living materials, Soft Matter 17 (4) (2021) 785–809.

[3] A. Rodrigo-Navarro, S. Sankaran, M.J. Dalby, A. del Campo, M. Salmeron-Sanchez, Engineered living biomaterials, Nat. Rev. Mater. 6 (12) (2021) 1175–1190.

[4] M.E. Inda-Webb, M. Jimenez, Q. Liu, N.V. Phan, J. Ahn, C. Steiger, A. Wentworth, A. Riaz, T. Zirtiloglu, K. Wong, K. Ishida, N. Fabian, J. Jenkins, J. Kuosmanen, W. Madani, R. McNally, Y. Lai, A. Hayward, M. Mimee, P. Nadeau, A. P. Chandrakasan, G. Traverso, R.T. Yazicigil, T.K. Lu, Sub-1.4 cm capsule for detecting labile inflammatory biomarkers in situ, Nature 620 (7973) (2023) 386.

[5] K. Schulz-Schönhagen, N. Lobsiger, W.J. Stark, Continuous production of a shelf-stable living material as a biosensor platform, Advanced Materials Technologies 4 (8) (2019) 1900266.

[6] M. Mimee, P. Nadeau, A. Hayward, S. Carim, S. Flanagan, L. Jerger, J. Collins, S. McDonnell, R. Swartwout, R.J. Citorik, V. Bulovic, R. Langer, G. Traverso, A. P. Chandrakasan, T.K. Lu, An ingestible bacterial-electronic system to monitor gastrointestinal health, Science 360 (6391) (2018) 915–918.

[7] M. Puertas-Bartolome, I. Gutierrez-Urrutia, L.L. Teruel-Enrico, C.N. Duong, K. Desai, S. Trujillo, C. Wittmann, A. Del Campo, Self-lubricating, living contact lenses, Adv. Mater. (2024) e2313848.

[8] Y.F. Lu, H.S. Li, J. Wang, M.Y. Yao, Y. Peng, T.F. Liu, Z. Li, G.X. Luo, J. Deng, Engineering bacteria-activated multifunctionalized hydrogel for promoting diabetic wound healing, Adv. Funct. Mater. 31 (48) (2021).

[9] T.C. Scanlon, S.M. Dostal, K.E. Griswold, A high-throughput screen for antibiotic drug discovery, Biotechnol. Bioeng. 111 (2) (2014) 232–243.

[10] K.Y. Qiu, I. Young, B.M. Woodburn, Y.R. Huang, A.C. Anselmo, Polymeric films for the encapsulation, storage, and tunable release of therapeutic microbes, Adv Healthc Mater 9 (6) (2020).

[11] A.M. Duraj-Thatte, N.M.D. Courchesne, P. Praveschotinunt, J. Rutledge, Y. Lee, J. M. Karp, N.S. Joshi, Genetically programmable self-regenerating bacterial hydrogels, Adv. Mater. 31 (40) (2019).

[12] H.H. Chen, F.S. Fu, Q.W. Chen, Y. Zhang, X.Z. Zhang, Two-pronged microbe delivery of nitric oxide and oxygen for diabetic wound healing, Nano Lett. 23 (12) (2023) 5595–5602.

[13] W.J. Wang, L. Zhang, Q.Q. Deng, Z.Q. Liu, J.S. Ren, X.G. Qu, Yeast@MOF bioreactor as a tumor metabolic symbiosis disruptor for the potent inhibition of metabolically heterogeneous tumors, Nano Today 42 (2022).

[14] X.Y. Liu, Y.Y. Yang, M.E. Inda, S.T. Lin, J.J. Wu, Y. Kim, X.Y. Chen, D.C. Ma, T. K. Lu, X.H. Zhao, Magnetic living hydrogels for intestinal localization, retention, and diagnosis, Adv. Funct. Mater. 31 (27) (2021).

[15] C.J. Ingham, A. Sprenkels, J. Bomer, D. Molenaar, A. van den Berg, J.E.T.V. Vlieg, W.M. de Vos, The micro-Petri dish, a million-well growth chip for the culture and high-throughput screening of microorganisms, P Natl Acad Sci USA 104 (46) (2007) 18217–18222.

[16] A. Bruns, H. Hoffelner, J. Overmann, A novel approach for high throughput cultivation assays and the isolation of planktonic bacteria, Fems Microbiol Ecol 45 (2) (2003) 161–171.

[17] P. Li, X.Q. Dou, C.L. Feng, M. Müller, M.W. Chang, M. Frettlöh, H. Schönherr, Isolated reporter bacteria in supramolecular hydrogel microwell arrays, Langmuir 33 (31) (2017) 7799–7809.

[18] N. Fattahi, P.A. Nieves-Otero, M. Masigol, A.J. van der Vlies, R.S. Jensen, R. R. Hansen, T.G. Platt, Photodegradable hydrogels for rapid screening, isolation, and genetic characterization of bacteria with rare phenotypes, Biomacromolecules 21 (8) (2020) 3140–3151.

[19] D.C. Meng, N. Mukhitov, D. Neitzey, M. Lucht, D.D. Schaak, C.A. Voigt, Rapid and simultaneous screening of pathway designs and chassis organisms, applied to engineered living materials, Metab. Eng. 66 (2021) 308–318.

[20] H.M. Nguyen, M.L. Pham, E.M. Stelzer, E. Plattner, R. Grabherr, G. Mathiesen, C. K. Peterbauer, D. Haltrich, T.H. Nguyen, Constitutive expression and cell-surface display of a bacterial beta-mannanase in Lactobacillus plantarum, Microb Cell Fact 18 (1) (2019) 76.

[21] J.P. Lynch, L. Goers, C.F. Lesser, Emerging strategies for engineering Nissle 1917-based therapeutics, Trends Pharmacol. Sci. 43 (9) (2022) 772–786.

[22] M.C. de Vries, E.E. Vaughan, M. Kleerebezem, W.M. de Vos, - : survival, functional and potential probiotic properties in the human intestinal tract, Int. Dairy J. 16 (9) (2006) 1018–1028.

[23] J.B. Sun, F. Gunzer, A.M. Westendorf, J. Buer, M. Scharfe, M. Jarek, F. Gössling, H. Blöcker, A.P. Zeng, Genomic peculiarity of coding sequences and metabolic potential of probiotic strain Nissle 1917 inferred from raw genome data, J. Biotechnol. 117 (2) (2005) 147–161.

[24] A.K. Yanamandra, S. Bhusari, A. Del Campo, S. Sankaran, B. Qu, In vitro evaluation of immune responses to bacterial hydrogels for the development of living therapeutic materials, Biomater. Adv. 153 (2023) 213554.

[25] E. Mutaflor, coli Stamm Nissle 1917: der medizinische Darmkeim | Mutaflor. https ://mutaflor.de/wissen/e-coli-stamm-nissle-1917/, 2022. (Accessed 24 April 2024).

[26] P. Health, Lactobacillus plantarum LPLDL®,The probiotic to support heart health. https://lpldl.com/. (Accessed 6 May 2024).

[27] T. Aoki, K. Kitazawa, H. Deguchi, C. Sotozono, Current evidence for on the ocular surface, Microorganisms 9 (2) (2021).

[28] J.A.P. Gomes, L. Frizon, V.F. Demeda, Ocular surface microbiome in health and disease, Asia-Pac J Ophthalmo 9 (6) (2020) 505–511.

[29] F. Riedel, M.P. Bartolomé, L.L.T. Enrico, C. Fink-Straube, C.N. Duong, F. Gherlone, Y. Huang, V. Valiante, A. Del Campo, S. Sankaran, Engineered living materials for the conversion of a low-cost food-grade precursor to a high-value flavonoid, Front. Bioeng. Biotechnol. 11 (2023) 1278002.

[30] N. Bühler, H.P. Haerri, M. Hofmann, C. Irrgang, A. Mühlebach, B. Müller, F. Stockinger, Nelfilcon A, a new material for contact lenses, Chimia 53 (6) (1999) 269–274.

[31] C. Gilbert, T.C. Tang, W. Ott, B.A. Dorr, W.M. Shaw, G.L. Sun, T.K. Lu, T. Ellis, Living materials with programmable functionalities grown from engineered microbial co-cultures, Nat. Mater. 20 (5) (2021) 691.

[32] L.Y. Li, C. Yang, B.L. Ma, S.J.J. Lu, J. Liu, Y.Y. Pan, X.Y. Wang, Y.L. Zhang, H. J. Wang, T. Sun, D. Liu, Hydrogel-encapsulated engineered microbial consortium as a photoautotrophic "living material" for promoting skin wound healing, Acs Appl Mater Inter (2023).

[33] D.X. Zhang, D.N. Zhong, J. Ouyang, J. He, Y.C. Qi, W. Chen, X.C. Zhang, W. Tao, M. Zhou, Microalgae-based oral microcarriers for gut microbiota homeostasis and intestinal protection in cancer radiotherapy, Nat. Commun. 13 (1) (2022).

[34] R.A. Soni, K. Sudhakar, R.S. Rana, Comparative study on the growth performance of Spirulina platensis on modifying culture media, Energy Rep. 5 (2019) 327–336.

[35] T.C. Tang, E. Tham, X.Y. Liu, K. Yehl, A.J. Rovner, H. Yuk, C. de la Fuente-Nunez, F.J. Isaacs, X.H. Zhao, T.K. Lu, Hydrogel-based biocontainment of bacteria for continuous sensing and computation, Nat. Chem. Biol. 17 (6) (2021) 724–731.

[36] S. Bhusari, J. Kim, K. Polizzi, S. Sankaran, A. del Campo, Encapsulation of bacteria in bilayer Pluronic thin film hydrogels: a safe format for engineered living materials, Biomater. Adv. 145 (2023).

[37] G. Wijesinghe, A. Dilhari, B. Gayani, N. Kottegoda, L. Samaranayake, M. Weerasekera, Influence of laboratory culture media on in vitro growth, adhesion, and biofilm formation of Pseudomonas aeruginosa and Staphylococcus aureus, Med. Princ. Pract. 28 (1) (2019) 28–35.

[38] Y. Rebai, L. Wagner, M. Gnaien, M.L. Hammer, M. Kapitan, M.J. Niemiec, W. Mami, A. Mosbah, E. Messadi, H. Mardassi, S. Vylkova, I.D. Jacobsen, S. Znaidi, Nissle 1917 antagonizes growth and protects intestinal cells from mediated damage, Microorganisms 11 (8) (2023).

[39] X.M. Luo, H.X. Song, J. Yang, B. Han, Y. Feng, Y.B. Leng, Z.Q. Chen, Encapsulation of strain Nissle 1917 in a chitosan-alginate matrix by combining layer-by-layer assembly with CaCl cross-linking for an effective treatment of inflammatory bowel diseases, Colloid Surface B 189 (2020).

[40] K. Lewis, Persister cells, Annu. Rev. Microbiol. 64 (2010) 357–372, 64, 2010.

[41] T.K. Wood, S.J. Knabel, B.W. Kwan, Bacterial persister cell formation and dormancy, Appl Environ Microb 79 (23) (2013) 7116–7121.

[42] B.F. Gilmore, S.P. Denyer, Hugo and Russell's Pharmaceutical Microbiology, John Wiley & Sons2023.

[43] Y. Watanabe, F. Nagai, M. Morotomi, Characterization of sp nov., an asaccharolytic, succinate-utilizing bacterium isolated from human feces, Appl Environ Microb 78 (2) (2012) 511–518.

[44] K. Hitomi, J.R.Y. Weng, B.W. Ying, Contribution of the genomic and nutritional differentiation to the spatial distribution of bacterial colonies, Front. Microbiol. 13 (2022).

[45] J.M. Chacón, W. Möbius, W.R. Harcombe, The spatial and metabolic basis of colony size variation, Isme J 12 (3) (2018) 669–680.

[46] L. Porfiri, J. Burtscher, R.T. Kangethe, D. Verhovsek, G. Cattoli, K.J. Domig, V. Wijewardana, Irradiated non-replicative lactic acid bacteria preserve metabolic activity while exhibiting diverse immune modulation, Front. Vet. Sci. 9 (2022).

[47] A. Grzywaczyk, A. Zdarta, K. Jankowska, A. Biadasz, J. Zdarta, T. Jesionowski, E. Kaczorek, W. Smulek, New biocomposite electrospun fiber/alginate hydrogel for probiotic bacteria immobilization, Materials 14 (14) (2021).

[48] M.Y. Jung, J. Lee, B. Park, H. Hwang, S.O. Sohn, S.H. Lee, H.I. Lim, H.W. Park, J. H. Lee, Applicability of a colorimetric method for evaluation of lactic acid bacteria with probiotic properties, Food Microbiol. 64 (2017) 33–38.

[49] W.C. Wu, Y.Y. Pu, H.L. Yao, H. Lin, J.L. Shi, Microbiotic nanomedicine for tumor-specific chemotherapy-synergized innate/adaptive antitumor immunity, Nano Today 42 (2022).

[50] M. Petaroudi, A. Rodrigo-Navarro, O. Dobre, M.J. Dalby, M. Salmeron-Sanchez, Living biointerfaces for the maintenance of mesenchymal stem cell phenotypes, Adv. Funct. Mater. 32 (32) (2022).

[51] P. Yang, Y. Chen, A.D. Gong, Development of a defined medium for Corynebacterium glutamicum using urea as nitrogen source, 3 Biotech 11 (9) (2021) 405.

[52] R. Shyamkumar, I.M. Moorthy, K. Ponmurugan, R. Baskar, Production of L-glutamic acid with Corynebacterium glutamicum (ncim 2168) and Pseudomonas reptilivora (ncim 2598): a study on immobilization and reusability, Avicenna J. Med. Biotechnol. 6 (3) (2014) 163–168.

[53] M. Inui, S. Murakami, S. Okino, H. Kawaguchi, A.A. Vertès, H. Yukawa, Metabolic analysis of during lactate and succinate productions under oxygen deprivation conditions, J Mol Microb Biotech 7 (4) (2004) 182–196.

[54] A.J. Phillips, L. Speedwell, Contact Lenses, Elsevier Health Sciences, 2018.

[55] B. McNeil, D. Archer, I. Giavasis, L. Harvey, Microbial Production of Food Ingredients, Enzymes and Nutraceuticals, Elsevier, 2013.

[56] J.J. Hay, A. Rodrigo-Navarro, M. Petaroudi, A.V. Bryksin, A.J. García, T.H. Barker, M.J. Dalby, M. Salmeron-Sanchez, Bacteria-based materials for stem cell engineering, Adv. Mater. 30 (43) (2018).